Journal of Materials Chemistry B

Accepted Manuscript

ROYAL SOCIETY OF CHEMISTRY

www.rsc.org/materialsB

Cite this: DOI: 10.1039/c0xx00000x

www.rsc.org/xxxxxx

ARTICLE TYPE

Preparation of Aggregation-Induced Emission Dots for Long-Term Two-Photon Cell Imaging

Qiang Ye‡, Shuangshuang Chen‡, Dandan Zhu, Xuemin Lu, and Qinghua Lu*

Received (in XXX, XXX) Xth XXXXXXXXX 20XX, Accepted Xth XXXXXXXXX 20XX

DOI: 10.1039/b000000x

Two-photon fluorescence imaging has attracted increasing interest in the biological and medical fields because of its low cell damage, high resolution, large imaging depth, and easy dynamic observation. A high-performance two-photon probe with long-term imaging capability was proposed for this imaging technology. In this work, a new two-photon probe compound was synthesized from tetraphenylethylene fluorogen with aggregation-induced emission. A phenyl-[phenyl-(1,2,5-thialdiazol)] amine group was induced to red-shift the absorption and emission wavelength of the compound. After self-assembly, fluorescent dots with aggregation-induced emission cores and hydrophobic shells terminated by –COOH were formed. Cell experiments proved that the 4-(7-(phenyl(4-(1,2,2triphenylvinyl)phenyl)amino)benzo[c][1,2,5]thiadiazol-4-yl)benzoic acid (TPECOOH) dots with red emission had good biocompatibility and excellent two-photon imaging ability. TPECOOH dots were used successfully in direct long-term cell imaging with a high efficiency. Even after twelve days, fluorescence imaging could still be observed in live HeLa cells.

Introduction

As a new kind of advanced nonlinear imaging method, two-photon fluorescence imaging microscopy has been used extensively in live cell and tissue imaging.[1, 2] Compared to single photon fluorescence, two-photon fluorescence depends quadratically on the excitation intensity, with high 3D spatiotemporal resolution resulting from that the fluorescent region can be confined to a volume of about cube of the excitation wavelength ($V \sim \lambda^3$) when excited by focusing laser.[3, 4] Furthermore, it also can be excited by near-infrared light (800–1100nm). Because water and blood are nearly transparent and non-scattering to near-infrared (IR) light, two-photon fluorescence imaging has attractive advantages such as low cell damage, high resolution ratio, a large imaging depth, and three-dimensional imaging capability.[5-9] Current imaging techniques have become powerful tools to observe and research the dynamic processes of living cells. However, the complexity and dynamic nature of biological phenomena requires fluorescence probes to have continuous non-invasive long-term imaging capacity.[10-16]

Several long-term fluorescence probes for cell imaging have been reported, including green fluorescent protein[17-19] and its variants for genetic cell tagging, inorganic semiconductor quantum dots,[20-24] or organic dye-doped nanoparticles[25]. Unfortunately, green fluorescent proteins possess some inherent drawbacks, for instance, susceptibility to enzyme degradation, small Stokes shifts, poor photostability, and interference with normal cell functions.[26-28] Although inorganic semiconductor quantum dots, which show bright emission and a high photo bleaching threshold under imaging conditions,[29] are used widely as fluorescent probes for direct cell labelling, the release of heavy metal ions results in high cytotoxicity, especially in an oxidative environment, and therefore hinders their future application.[30-32] Organic dye-doped nanoparticles have a longer cellular retention time, intense fluorescence, and lower exocytosis rate.[33] However, the majority of commercially available organic dyes have a non-specific contrast agent transfer (low Stokes shift) and aggregation-caused quenching.[34]

Direct cell labelling by organic or inorganic fluorescent materials without genetic modification of cells has drawn increased attention recently.[35, 36] However, the currently used fluorescent probes exhibit serious disadvantages of short cell retention time[37] or aggregation-caused quenching problems, and hinder their application in long-term cell imaging. Recently, Tang and co-workers developed a series of organic luminogens based on tetraphenylethene (TPE) fluorogens, which showed an extraordinary aggregation-induced emission (AIE) feature and may overcome the aggregation-caused quenching problem.[38-40]

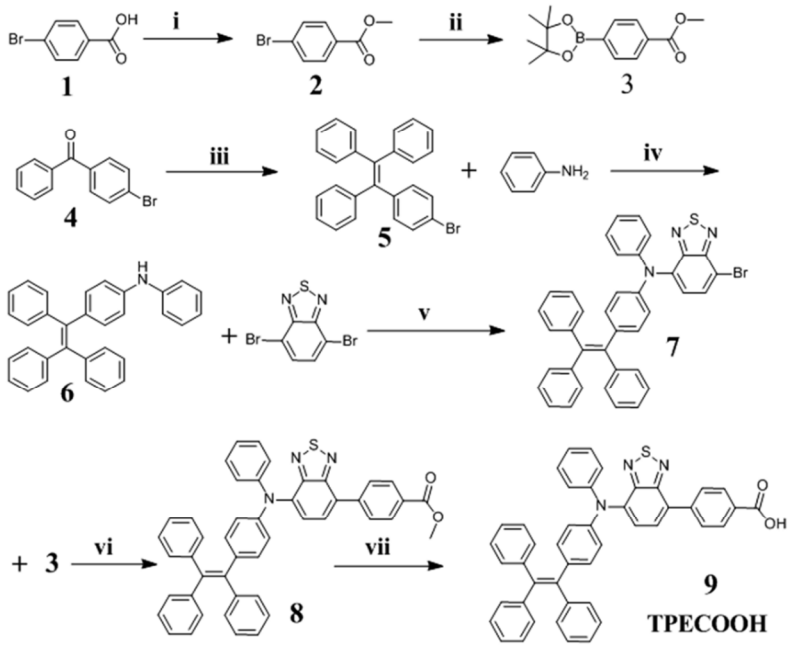

Scheme 1. Synthetic routes of TPECOOH. [α] Conditions: (i) sulfuric acid, CH_3OH, reflux, 24 h. (ii) bis(pinacolato)diboron, $PdCl_2$(dppf), CH_3COOK, DMF, reflux, 6 h. (iii) a) n-BuLi, THF, -5°C, 10 h, b) p-toluene sulfonic acid, toluene, reflux, overnight. (iv) $Pd_2(dba)_3$, tri-tert-butylphosphine, sodium mtert-butoxide, toluene, reflux, 24 h. (v) $Pd(OAc)_2$, tri-tert- butylphosphine, Cs_2CO_3, toluene, reflux, 24 h. (vi) $Pd(PPh_3)_4$, K_2CO_3 (2 M, aq.), THF/ ethanol/ H_2O, 80°C, 12 h. (vii) HCl, THF/water, 70 °C, 24 h.

Inspired by their work, we designed and synthesised a new red emissive AIE compound, 4-(7-(phenyl(4-(1,2,2triphenylvinyl)phenyl)amino)benzo[c][1,2,5]thiadiazol-4-yl)benzoic acid (TPECOOH), which is derived from tetraphenylethene. The introduction of the pheny-[phenyl-(1,2,5-thialdiazol)] amine group favours the red shift of the absorption of TPE because of molecular conjugation, thereby reducing the excitation wavelength and obtaining red fluorescence emission. We tried to use a terminal carboxyl group to improve the self-assembly capability of the fluorescent compound and the stability of assembled dots in aqueous media, and to provide a certain affinity with cell membranes. The TPECOOH dots showed good one-photon imaging with a large Stokes shift of 142 nm, and brilliant two-photon imaging ability excited by light of the near-IR region (800–1100 nm). The dots also exhibited an excellent biocompatibility and a high efficiency in direct long-term cell imaging.

Experimental

Materials

All reagents were purchased from J&K Scientific Co. and used without further purification. All solvents were purchased from National Pharmaceutical Group Chemical Reagent Co. Analytical grade dimethyl formamide was purified by distillation under an inert nitrogen atmosphere. Tetrahydrofuran (THF) was distilled from sodium/benzophenone. Water was purified with a Hitech system to reach a resistivity of above 18.2 MΩ·cm. HeLa cells were obtained from the Cell Resource Centre of Life Sciences in Shanghai, China. Bovine serum albumin (66 kD, > 98%), fetal bovine serum, and Dulbecco's modified Eagle medium were obtained from Gibco BRL. Cellular cytotoxicity evaluating reagent (Cell Counting Kit-8) and all other cell culture reagents were purchased from the Beyotime Institute of Biotechnology.

Characterization

Nuclear magnetic resonance (NMR) spectra were recorded using a MERCURY plus 400 (Varian, Inc., USA) nuclear magnetic resonance spectrometer in deuterated chloroform ($CDCl_3$) using tetramethylsilane (δ=0) as internal reference. High-resolution mass-spectrometric analysis was performed on a Fourier transform ion cyclotron resonance mass spectrometer (MS) SolariX-70FT-MS (Bruker Daltonics, Germany) operating in MALDI-mode. The ultraviolet/visible (UV/Vis) spectra were measured on a Lambda 20 UV/Vis spectrometer (Perkin Elmer, Inc., USA). Fluorescence spectra were measured using an LS 50B spectrometer (Perkin Elmer, Inc., USA). Quantum yield measurements were carried out on a QM/TM steady-state and time-resolved fluorescence spectrofluorometer (PTI Company, USA). Diameter analysis of the TPECOOH dots was determined by a ZS90 (Malvern Instruments) dynamic light scanning (DLS) instrument, and all samples were measured at a scattering angle of 90°. Transmission electron microscope (TEM) images were recorded by a Tecnai G2 spirit Biotwin microscope (FEI Company, USA) at an accelerating voltage of 120 kV. Cell imaging observations were performed on an inverted fluorescence microscope (IX 71, Olympus) equipped with a charge-coupled device camera. One- and two-photon fluorescent images were taken on a Leica TCS SP5 confocal laser scanning microscope (Leica Microsystems, Germany).

Synthesis and characterization of TPECOOH compound

The TPECOOH synthesis routes are shown in Scheme 1. The detailed synthetic processes are as follows.

Compound 2. Sulfuric acid (0.5 mL) was added to a suspension of compound **1** (5 g) in anhydrous methanol (50 mL). The mixture was stirred at 80°C for 12 h and then the residual methanol was removed under reduced pressure. The residue was recrystallized from dichloromethane (CH_2Cl_2) to give a white powder (4.97 g, 93%). ^{1}H NMR (400 MHz, $CDCl_3$) δ 8.01–7.83 (m, 2H; Ar-*H*), 7.67–7.51 (m, 2H; Ar-*H*), 3.92 (dd, J = 7.9, 2.7 Hz, 3H; OCH_3).

Compound 3. Pd(dppf)Cl_2 (400 mg, 0.48 mmol) was added to a mixture of compound **2** (3.00 g, 14 mmol), bis(pinacolato)diboron (4 g, 16 mmol) and KOAc (4.1 g, 42 mmol) in 60 mL of dimethyl formamide under argon. The mixture was refluxed overnight. After being quenched with aqueous ammonium chloride, the mixture was extracted with CH_2Cl_2. The combined organic layer was washed with brine, and dried over anhydrous sodium sulfate. After removal of the solvent at reduced pressure, the residue was purified by column chromatography (silica gel, ethyl acetate/petroleum ether (PE) = 1/15 v/v) to obtain a white solid compound **3** (3.18 g, yield: 87%). ^{1}H NMR (400 MHz, $CDCl_3$) δ 8.08–7.97 (m, 2H; Ar-*H*), 7.92–7.82 (m, 2H; Ar-*H*), 3.93–3.89 (m, 3H; OCH_3), 1.37–1.33 (m, 12H; OC(CH_3)$_2$).

Compound 5. A 2.5 M solution of n-butyllithium in hexane (18 mL, 45 mmol) was added to a solution of diphenylmethane (6.75 g, 40 mmol) in anhydrous tetrahydrofuran (50 mL) at -5°C under argon. After stirring for 2 h, 4-bromobenzophenone (10.44 g, 40 mmol) was added and the reaction mixture was stirred for 10 h to allow the temperature to rise gradually to room temperature. The reaction was quenched with an aqueous solution of ammonium chloride, and the mixture was extracted with CH_2Cl_2. The organic layer was evaporated after drying with anhydrous sodium sulfate and the resulting crude hydroxyl intermediate was dissolved in toluene (100 mL). p-Toluenesulfonic acid (1.0 g, 5.85 mmol) was added, and the mixture was refluxed for 12 h and cooled to room temperature. The mixture was evaporated and the crude product was purified by silica gel column chromatography using DCM/PE (v/v = 1/10) as eluent to yield compound **5** as a white powder (13.6 g, 83%). ^{1}H NMR (400 MHz, $CDCl_3$) δ 7.25–7.18 (m, 2H; Ar-*H*), 7.12 (ddd, J = 6.6, 5.3, 3.3 Hz, 9H; Ar-*H*), 7.06–6.98 (m, 6H; Ar-*H*;), 6.93–6.87 (m, 2H; Ar-*H*).

Compound 6. Tri-tert-butylphosphine (26.3 mg, 0.13 mmol), $Pd_2(dba)_3$ (0.1 g, 0.11 mmol), and sodium tert-butoxide (0.96 g, 10 mmol) in dry toluene (30 mL) were added to a mixture of compound **5** (3.28 g, 8 mmol) and aniline (0.94 g, 10 mmol) under argon. The mixture was stirred at 110°C for 24 h. After solvent removal, water (50 mL) and DCM (100 mL) were added. The organic layer was separated and washed with brine, dried over anhydrous magnesium sulfate and evaporated to dryness under reduced pressure. The crude product was purified by column chromatography on silica gel using DCM/PE (v/v = 1/6) as eluent to yield **6** as a pale yellow solid (2.1 g, 62%). ^{1}H NMR (400 MHz, $CDCl_3$) δ 7.25–7.20 (m, 2H; Ar-*H*), 7.16–6.99 (m,17H; Ar-*H*), 6.94–6.86 (m, 3H; Ar-*H*), 6.80 (d, J = 8.6 Hz, 2H; Ar-*H*), 5.65 (s, 1H; N*H*).

Compound 7. Compound **7** was prepared from **6** (1.26 g, 3 mmol), 4,7-dibromo-2,1,3-benzothidiazole (2.6 g, 9 mmol), Cs_2CO_3 (2.93 g, 9 mmol), $Pd(OAc)_2$ (60.7 mg, 0.3 mmol), and tri-tert-butylphosphine (0.1 g, 0.5 mmol), following the same procedure described for the synthesis of **6** to yield **7** as a red solid (1.05 g, 55%). ^{1}H NMR (400 MHz, $CDCl_3$) δ 7.66 (d, J = 8.0 Hz, 1H; Ar-*H*), 7.24 (dd, J = 6.1, 5.2 Hz, 2H; Ar-*H*), 7.17–6.96 (m, 19H; Ar-*H*), 6.92–6.87 (m, 2H; Ar-*H*), 6.78–6.73 (m, 2H; Ar-*H*).

Compound 8 (TPECOOCH$_3$). Into a solution of compound **7** (0.8 g, 1.25 mmol) and compound **3** (0.34 g, 1.3 mmol) in 20 mL potassium carbonate (2 M, aq.) mixed with 60 mL THF and 20 mL ethanol, tetrakis(triphenylphosphine)palladium(0) (72 mg, 0.063 mmol) was added under argon atmosphere. The reaction temperature was increased to 80°C and the mixture was stirred for 24 h. The solution was concentrated by a rotary evaporator and extracted with CH_2Cl_2. The organic layer was separated and washed with brine, dried over anhydrous magnesium sulfate, and evaporated to dryness under reduced pressure. The crude product was purified using a silica-gel column with DCM/PE (v/v = 1/6) as eluent. Product **8** was obtained with 75% yield (0.65 g). ^{1}H NMR (400 MHz, $CDCl_3$) δ 8.21 (d, J = 8.4 Hz, 2H; Ar-*H*), 8.05 (t, J = 6.5 Hz, 2H; Ar-*H*), 7.66 (d, J = 7.8 Hz, 1H; Ar-*H*), 7.32–7.28 (m, 2H; Ar-*H*), 7.23–7.05 (m, 19H; Ar-*H*), 6.96 (d, J = 8.6 Hz, 2H; Ar-*H*), 6.84 (d, J = 8.6 Hz, 2H; Ar-*H*), 4.00–3.98 (m, 3H; OCH_3).

Compound 9 (TPECOOH). Compound **8** (0.5 g) was dissolved in 10 mL THF, then 10 mL water and 2 mL concentrated hydrochloric acid were added. The solution was placed in a nitrogen atmosphere and heated to 70°C with vigorous stirring for 48 h. The solution was concentrated by a rotary evaporator and extracted with CH_2Cl_2. The organic layer was separated and washed with brine, dried over anhydrous magnesium sulfate, and evaporated to dryness under reduced pressure. The crude product was recrystallized from DCM to give **9** as a red powder (0.39 g, 79%). ^{1}H NMR (400 MHz, $CDCl_3$) δ 8.24–8.15 (m, 4H; Ar-*H*), 7.92 (ddd, J = 9.1, 7.0, 2.3 Hz, 2H; Ar-*H*), 7.35–7.05 (m, 19H; Ar-*H*), 7.02–6.91 (m, 3H; Ar-*H*), 6.90–6.82 (m, 2H; Ar-*H*). ^{13}C NMR (101 MHz, $CDCl_3$) δ 171.34 (s), 154.59 (s), 151.13 (s), 147.23 (s), 145.70 (s), 143.97 (s), 143.56 (d, J = 18.9 Hz), 142.84 (s), 140.92 (s), 140.54 (s), 140.02 (s), 139.16 (s), 132.26 (s), 131.70–131.12 (m), 130.52 (s), 129.27 (s), 128.97 (s), 128.21 (s), 127.67 (d, J = 2.7 Hz), 127.42 (s), 126.45 (d, J = 7.2 Hz), 124.47 (s), 123.56 (d, J = 48.8 Hz), 123.31–123.13 (m), 122.55 (s). High-resolution MS (MALDI, m/z): [M+] calcd for C45H31N3O2S: 677.81; Found: 677.212816.

Preparation of TPECOOH dots

The as-prepared TPECOOH (1 mg) was dissolved in 0.5 mL THF, and then 0.5 mL of the sample solution (2 mg/mL) was added dropwise into 5 mL of water with intensive stirring. The mixture was stirred vigorously at room temperature for 24 h. The TPECOOH molecules aggregated to form AIE dots that were then suspended in water.

Cell culture

HeLa cells were cultured in Dulbecco's modified Eagle medium containing 10% fetal bovine serum and antibiotics (50 units/mL penicillin and 50 units/mL stretomycin) at 37°C in a humidified atmosphere containing 5% CO_2. The cells were seeded in 6-well plates at 10^5 cells per well and cultured for 6 h to reach confluence. TPECOOH dots dispersed in water (5 μg/mL) were

added for cell imaging. Twelve hours later, after medium removal and washing twice with phosphate buffer solution, cell imaging was recorded using a fluorescence microscope.

Cytotoxicity study

The cytotoxicity of the TPECOOH dots was determined using a cell counting kit (CCK)-8. The HeLa cells were seeded in 96-well plates at 10^4 cells per mL. After cell spreading for 80% confluence, TPECOOH dots were added at 0.01, 0.1, 1, 5, 10, and 50 μg/mL. The well without TPECOOH dots was set as a control. To eliminate the influence of TPECOOH dots, the same TPECOOH dot solution was added into the well without cells. After incubating the cells for different periods of time, the absorbance at 450 nm was recorded using a microplate reader (BIO-RED).

One- and two-photon fluorescent cellular imaging

For one- and two-photon fluorescence imaging, HeLa cells were seeded onto the coverslip for 6 h and were added with 5 μg/mL TPECOOH dots. After being incubated for 12 h, samples were fixed with 2.5% glutaraldehyde for 5 min, and the coverslip was sealed onto the glass slide. Two-photon fluorescent images were taken using a confocal laser scanning microscope (Leica TCS SP5) with excitation at 880 nm. For comparison, one-photon fluorescence images were also measured with an excitation at 488 nm. Cells were exposed to the laser for 20 min to evaluate the resistance to photobleaching.

Results and discussion

Synthesis and characterization of TPECOOH

TPECOOH was synthesized as shown in Scheme 1. NMR and MS were used to confirm the molecular structure of TPECOOH. The ^{1}H NMR, ^{13}C NMR, and high-resolution MS results for the TPECOOH in Figures S7–S9, respectively, show that the TPECOOH was synthesized successfully.

Optical properties of TPECOOH

The optical properties of TPECOOH were studied by UV/Vis and fluorescence spectra. Figure 1a shows the UV/Vis absorption spectrum of the TPECOOH dots suspended in water, which was similar to that of the TPECOOH solution in THF (see Fig. S10). The TPECOOH presented two absorption peaks at 310 and 488 nm, respectively. Figure 1b shows the one-photon luminescence spectra of the TPECOOH molecule dissolved in THF and THF-water mixtures with different water proportions. Almost no fluorescence emission was detected when the concentration of water, as a poor solvent, was less than 30%. When the water concentration exceeded 50%, TPECOOH aggregation occurred and the free rotation of tetraphenylethene inside the aggregate was restricted. Therefore, the non-radiative decay channels were blocked, which lead to obvious fluorescence emission at 630 nm. The emission intensity increased with increase in water concentration. This phenomenon can be attributed to the AIE effect of TPECOOH. The inset in Fig. 1b shows the fluorescence emission of TPECOOH in THF and THF/water (10/90) solution, respectively at 365 nm irradiation using a commercially available UV lamp. Compared with the absorption peak at 488 nm in the UV/Vis spectra, the TPECOOH suspension has a maximum emission at 630 nm with a large Stokes shift of 142 nm. The TPECOOH suspension had a fluorescence quantum yield (Φ_f) of ~30%.

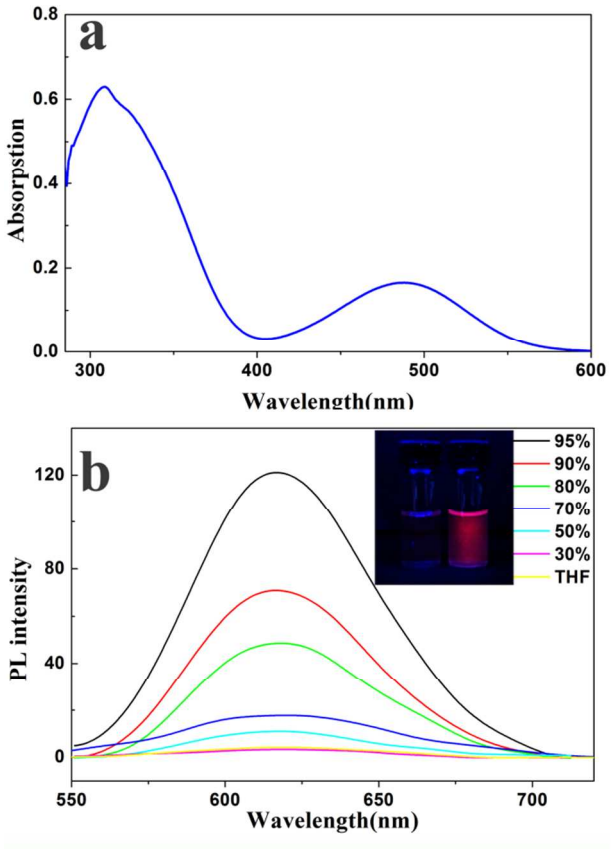

Figure 1. a) UV/Vis absorption spectrum of TPECOOH dots suspended in water. b) Photoluminescence spectra (PL) of TPECOOH in THF/water mixtures with different water fractions. (Concentration of TPECOOH: 10^{-5} M, excitation wavelength: 510 nm).

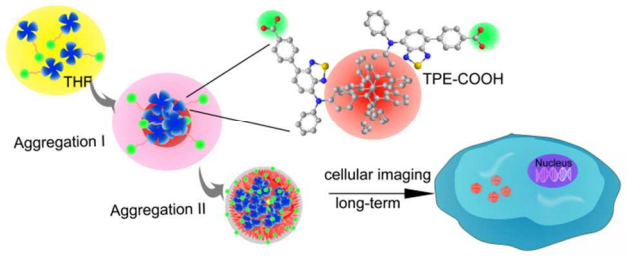

Figure 2. Schematic illustration of fabrication of AIE-dots for application in long-term cell imaging.

Fabrication and characterization of TPECOOH dots

The fabrication of TPECOOH dots is illustrated in Fig. 2. The addition of TPECOOH in THF into the aqueous media resulted in the hydrophobic–hydrophilic balance force promoting TPECOOH molecule aggregation and the formation of TPECOOH dots with hydrophilic shells terminated by a –COOH moiety, which presented strong fluorescence. The morphology of the AIE dots is shown by the TEM images in Fig. 3a, which exhibit a spherical structure with good monodispersity and 40–60 nm diameter. The inset image shows a magnification of the

TPECOOH dots. DLS measurements also show that the TPECOOH dots at 0.1 mg/mL in aqueous solution had a hydrodynamic diameter of approximately 68 nm with a polydispersity index of 0.26 (Fig. 3b). Because of the formation of a hydration layer on the dots, the diameter of the dots obtained from DLS measurements was slightly larger than that from TEM.

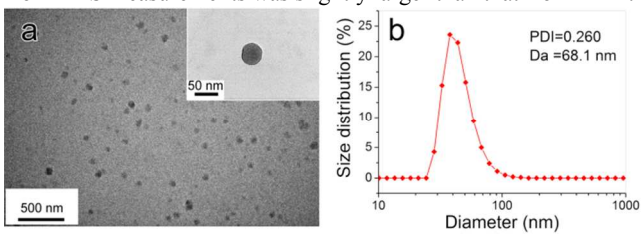

Figure 3. a) TEM image of TPECOOH dots, inset: magnification image. b) Diameter distribution of TPECOOH dots obtained by DLS. Polydispersity index (PDI ~0.260), and average size (Da ~68 nm).

Cytotoxicity and photostability

The biocompatibility of fluorescence dots is of vital significance in biomedical application. A cytotoxicity evaluation of the TPECOOH dots was performed using a cell counting kit (CCK)-8. The results are shown in Fig. 4a. Cell viabilities over such a wide concentration range had no obvious change over 24 h incubation. Even when cultured for 48 h at 50 μg/mL, the cell viability was more than 85%, which indicates that the TPECOOH dots have a low cytotoxicity and good biocompatibility. Most probe molecules are photobleaching and are quenched easily under laser irradiation, which limits their application. In this study, the photostability of the TPECOOH dots was investigated. Figure 4b show the change in fluorescence intensity of the TPECOOH dots that were exposed to continuous laser irradiation of 488 nm for 20 min. Only a slight decrease in fluorescence occurred, but no obvious photobleaching was observed, which implies excellent photostability. The good biocompatibility and photostability endow TPECOOH dots with great potential for cell imaging and long-term tracing.

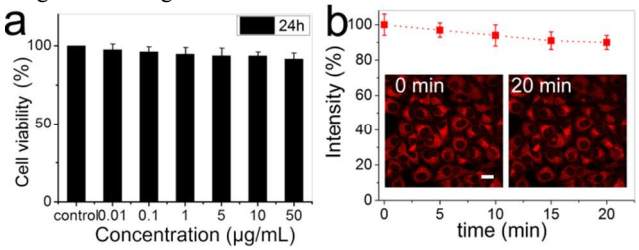

Figure 4. a) Cell viability of TPECOOH dots at different concentrations cultured for 24 h. b) Photostability of TPECOOH dots under laser irradiation at 488 nm for 20 min (emission filter wavelengths was 620 nm when excited by 488 nm with laser power at 2 mW .), inset: initial confocal images taken before (left, 0 min) and after (right, 20 min) irradiation, respectively. Scale bar = 25 μm.

Live cell tracing

The requirement of long-term fluorescent probes has been recognized in recent years for applications in clinical cancer diagnosis. Here, HeLa cells were cultured with TPECOOH at a concentration of 5 μg/mL. After being cultured for 12 h, the culture medium was removed and rinsed twice with phosphate buffer solution to remove the non-adsorbed TPECOOH dots. The new culture medium was added again to provide nutrition for cells. Fluorescence images taken by normal fluorescence microscopy are shown in Fig. 5. Figure 5a was taken after 2 days, and shows excellent fluorescence. Fluorescence intensity decreased with time because of cell proliferation, in which the TPECOOH dots divide into daughter cells. Fluorescence can still be observed after 12 days, which indicates that the TPECOOH dots are appropriate for long-term tracing.

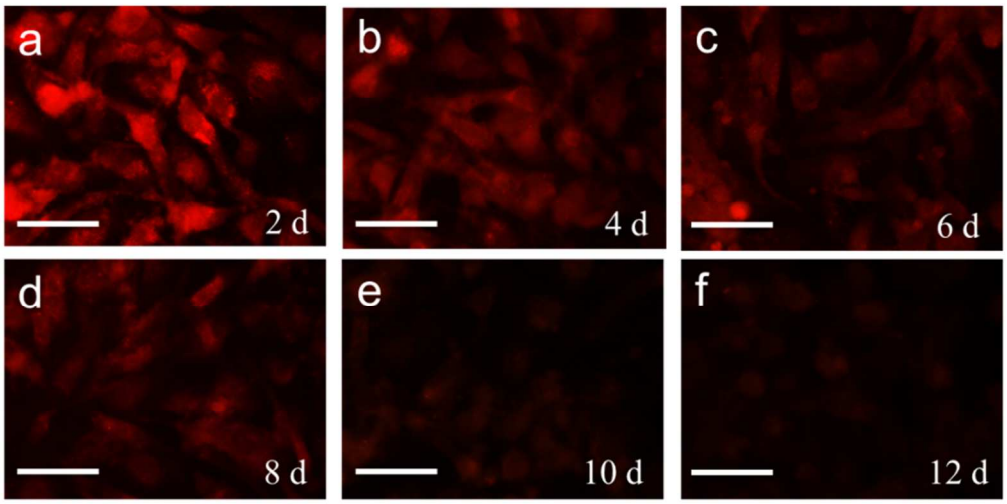

Figure 5. Long-term cell tracing images of TPECOOH dots (from 2 to 12 days). Excitation wavelength: 545 nm. Scale bar = 100 μm.

For comparison, the cell imaging capability of compound **8** was also evaluated. However, the hydrophobic dots of compound **8** cannot be used to label the cell even after being cultured for 48 h. The hydrophobic nanoparticles were not taken up into the cell, possibly because of the lack of aqueous stability that results in precipitation and a low affinity with the cell membrane (Fig. S11). This comparison verified our hypothesis that for cell imaging, the intrinsic balance between hydrophobicity and hydrophilicity of the fluorescence molecule plays a crucial rule in labeling and tracing cells, and the good affinity of TPECOOH dots with cell membranes originates from the hydrophilic carboxyl group.

Two-photon fluorescence properties

One-photon fluorescence generally acquires short-wavelength

irradiation, which may be harmful to cells and is easily absorbed by water and scattered because of the Rayleigh scattering effect. However, two-photon fluorescence can overcome these shortcomings since excitation occurs in the near-IR region (800–1100 nm), which means less light is absorbed by and scattered in water. Therefore, near-IR light-excited two-photon fluorescence has advantages for cell imaging.[7, 41] In this study, we investigated the two-photon fluorescence of TPECOOH dots for cell imaging. After incubating HeLa cells with TPECOOH dots at 5 μg/mL for 24 h, an 880 nm laser was used as excitation source to perform two-photon fluorescence. HeLa cells labeled by TPECOOH dots showed intense two-photon fluorescence (Fig. 6). Cytoplasm and cell borders could be recognized clearly when the cell nucleus was not labeled. The magnification image of a single cell (Fig. 6b) provided additional details on the cells. Therefore, TPECOOH dots are promising candidates in two-photon microscopic bio-imaging.

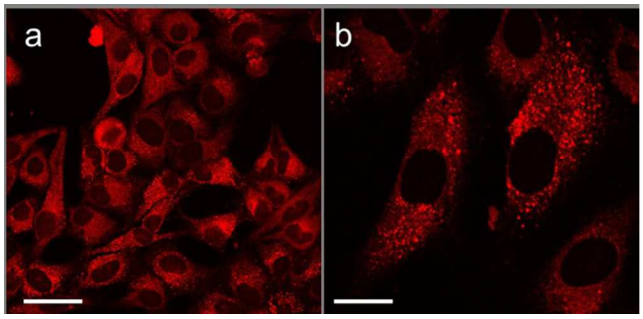

Figure 6. Two-photon confocal laser scanning microscopy images (excited at 880 nm). a) Scale bar = 50 μm. b) Magnification of (a), scale bar = 25 μm.

Conclusions

In summary, TPECOOH with a hydrophobic TPE fluorogen domain and hydrophilic shell terminated by carboxyl groups was designed and synthesized. The TPECOOH dots could be fabricated easily by aggregation of TPECOOH molecules dispersed in a THF/water mixture. They showed good monodispersity, significant aggregation-induced emission properties in aqueous solution, and were able to enter cells because of the good affinity of the carboxyl group for the cell membrane. Our studies show that the TPECOOH dots had a red emission, good two-photon imaging ability, low toxicity, good photostability, large Stokes shift, and biocompatible properties. Furthermore, they performed very well in direct long-term cell imaging. The AIE dots may have great potential in direct long-term cell imaging.

Acknowledgements

This research was supported by 973 Projects (2012CB933803, 2014CB643605), the National Science Fund for Distinguished Young Scholars (50925310), the National Science Foundation of China (21374060, 51173103), and Excellent Academic Leaders of Shanghai (11XD1403000).

Notes and references

Address, School of Chemistry and Chemical Engineering, Shanghai Jiao Tong University, Shanghai 200240, China. E-mail: qhlu@sjtu.edu.cn

† Electronic Supplementary Information (ESI) available: [NMR spectra of all the compounds, MS spectrum of compound **9** TPECOOH, UV/Vis spectrum of TEPCOOH in THF and the cell imaging evaluation of comparison compound **8**.]. See DOI: 10.1039/b000000x/

‡ These authors contributed equally to this work.

1. M. J. Miller, S. H. Wei, I. Parker and M. D. Cahalan, *Science*, 2002, **296**, 1869-1873.
2. C. Stosiek, O. Garaschuk, K. Holthoff and A. Konnerth, *P. Natl. Acad. Sci.* , 2003, **100**, 7319-7324.
3. X. Zhang, X. Yu, Y. Sun, W. He, Y. Wu, Y. Feng, X. Tao and M. Jiang, *Opt. Mater.*, 2006, **28**, 1366-1371.
4. P. W. Wiseman, J. A. Squier, M. H. Ellisman and K. R. Wilson, *J. Microsc.* , 2000, **200**, 14-25.
5. P. Theer, M. T. Hasan and W. Denk, *Opt. Lett.*, 2003, **28**, 1022-1024.
6. F. Helmchen and W. Denk, *Nat. Methods*, 2005, **2**, 932-940.
7. D. Ding, C. C. Goh, G. Feng, Z. Zhao, J. Liu, R. Liu, N. Tomczak, J. Geng, B. Z. Tang, L. G. Ng and B. Liu, *Adv. Mater.*, 2013, **25**, 6083-6088.
8. G. Tong, J. Wang, R. Wang, X. Guo, L. He, F. Qiu, G. Wang, B. Zhu, X. Zhu and T. Liu, *J. Mater. Chem. B*, 2015, **3**, 700-706.
9. J. Croissant, M. Maynadier, A. Gallud, H. P. N'Dongo, J. L. Nyalosaso, G. Derrien, C. Charnay, J. O. Durand, L. Raehm, F. Serein-Spirau, N. Cheminet, T. Jarrosson, O. Mongin, M. Blanchard-Desce, M. Gary-Bobo, M. Garcia, J. Lu, F. Tamanoi, D. Tarn, T. M. Guardado-Alvarez and J. I. Zink, *Angew. Chem. Int. Edit.*, 2013, **52**, 13813-13817.
10. D. J. Stephens and V. J. Allan, *Science*, 2003, **300**, 82-86.
11. X. Y. Wu, H. J. Liu, J. Q. Liu, K. N. Haley, J. A. Treadway, J. P. Larson, N. F. Ge, F. Peale and M. P. Bruchez, *Nat. Biotechnol.*, 2003, **21**, 41-46.
12. H. Q. Ly, J. V. Frangioni and R. J. Hajjar, *Nat. Clin. Pract. Cardiovasc. Med.*, 2008, **5**, S96-S102.
13. E. J. Sutton, T. D. Henning, B. J. Pichler, C. Bremer and H. E. Daldrup-Link, *Eur. Radiol.*, 2008, **18**, 2021-2032.
14. N. M. Idris, Z. Q. Li, L. Ye, E. K. W. Sim, R. Mahendran, P. C. L. Ho and Y. Zhang, *Biomaterials*, 2009, **30**, 5104-5113.
15. M. F. Kircher, S. S. Gambhir and J. Grimm, *Nat. Rev. Clin. Oncol.*, 2011, **8**, 677-688.
16. A. Taylor, K. M. Wilson, P. Murray, D. G. Fernig and R. Levy, *Chem. Soc. Rev.*, 2012, **41**, 2707-2717.
17. S. Wang and T. Hazelrigg, *Nature*, 1994, **369**, 400-403.
18. C. J. Daly and J. C. McGrath, *Pharmacol. Ther.*, 2003, **100**, 101-118.
19. R. Y. Tsien, *Angew. Chem. Int. Edit.*, 2009, **48**, 5612-5626.
20. A. Priyam, N. M. Idris and Y. Zhang, *J. Mater. Chem.*, 2012, **22**, 960-965.
21. X. H. Gao, Y. Y. Cui, R. M. Levenson, L. W. K. Chung and S. M. Nie, *Nat. Biotechnol.*, 2004, **22**, 969-976.
22. S. Kim, H. E. Pudavar, A. Bonoiu and P. N. Prasad, *Adv. Mater.*, 2007, **19**, 3791-3795.
23. M. Li, J. W. Y. Lam, F. Mahtab, S. Chen, W. Zhang, Y. Hong, J. Xiong, Q. Zheng and B. Z. Tang, *J. Mater. Chem. B*, 2013, **1**, 676-684.
24. J. Wang, D. X. Ye, G. H. Liang, J. Chang, J. L. Kong and J. Y. Chen, *J. Mater. Chem. B*, 2014, **2**, 4338-4345.
25. B. D. Chithrani and W. C. Chan, *Nano Lett.*, 2007, **7**, 1542-1550.
26. Y. G. Meng, J. Liang, W. L. Wong and V. Chisholm, *Gene*, 2000, **242**, 201-207.
27. J. K. Jaiswal, E. R. Goldman, H. Mattoussi and S. M. Simon, *Nat. Methods*, 2004, **1**, 73-78.
28. B. S. Shah, P. A. Clark, E. K. Moioli, M. A. Stroscio and J. J. Mao, *Nano Lett.*, 2007, **7**, 3071-3079.
29. J. Qian, D. Wang, F. H. Cai, Q. Q. Zhan, Y. L. Wang and S. L. He, *Biomaterials*, 2012, **33**, 4851-4860.
30. S. J. Cho, D. Maysinger, M. Jain, B. Röder, S. Hackbarth and

F. M. Winnik, *Langmuir*, 2007, **23**, 1974-1980.
31. M. De, P. S. Ghosh and V. M. Rotello, *Adv. Mater.*, 2008, **20**, 4225-4241.
32. D. W. Domaille, E. L. Que and C. J. Chang, *Nat. Chem. Biol.*, 2008, **4**, 168-175.
33. A. Palma, L. A. Alvarez, D. Scholz, D. O. Frimannsson, M. Grossi, S. J. Quinn and D. F. O'Shea, *J. Am. Chem. Soc.*, 2011, **133**, 19618-19621.
34. M. Shimizu and T. Hiyama, *Chem. Asian J.*, 2010, **5**, 1516-1531.
35. Y. Gao, Y. Cui, J. K. Chan and C. Xu, *Am. J. Nucl. Med. Mol. Imaging*, 2013, **3**, 232-246.
36. X. Yuan, M. I. Setyawati, A. S. Tan, C. N. Ong, D. T. Leong and J. P. Xie, *NPG Asia Mater.*, 2013, **5**, e39.
37. K. M. Marks and G. P. Nolan, *Nat. Methods*, 2006, **3**, 591-596.
38. J. D. Luo, Z. L. Xie, J. W. Y. Lam, L. Cheng, H. Y. Chen, C. F. Qiu, H. S. Kwok, X. W. Zhan, Y. Q. Liu, D. B. Zhu and B. Z. Tang, *Chem. Commun.*, 2001, 1740-1741.
39. Y. Hong, J. W. Y. Lam and B. Z. Tang, *Chem. Commun.*, 2009, 4332-4353.
40. Y. Hong, J. W. Y. Lam and B. Z. Tang, *Chem. Soc. Rev.*, 2011, **40**, 5361-5388.
41. K. Li, Y. Jiang, D. Ding, X. Zhang, Y. Liu, J. Hua, S.-S. Feng and B. Liu, *Chem. Commun.*, 2011, **47**, 7323-7325.

Table of contents

A high-performance two-photon probe with long-term cellular imaging capability was synthesized from an amphiphilic aggregation-induced emission molecule derived from tetraphenylethylene fluorogen.